JACS
JOURNAL OF THE AMERICAN CHEMICAL SOCIETY

COMMUNICATION

pubs.acs.org/JACS

Large-Area Graphene Single Crystals Grown by Low-Pressure Chemical Vapor Deposition of Methane on Copper

Xuesong Li,[†] Carl W. Magnuson,[†] Archana Venugopal,[‡] Rudolf M. Tromp,[§] James B. Hannon,[§] Eric M. Vogel,[‡] Luigi Colombo,[*,∥] and Rodney S. Ruoff[*,†]

[†]Department of Mechanical Engineering and the Texas Materials Institute, The University of Texas at Austin, 1 University Station C2200, Austin, Texas 78712-0292, United States

[‡]Department of Electrical Engineering, The University of Texas at Dallas, Richardson, Texas 75080, United States

[§]IBM T. J. Watson Research Center, Yorktown Heights, New York 10598, United States

[∥]Texas Instruments, 13121 TI Boulevard, Dallas, Texas 75243, United States

ABSTRACT: Graphene single crystals with dimensions of up to 0.5 mm on a side were grown by low-pressure chemical vapor deposition in copper-foil enclosures using methane as a precursor. Low-energy electron microscopy analysis showed that the large graphene domains had a single crystallographic orientation, with an occasional domain having two orientations. Raman spectroscopy revealed the graphene single crystals to be uniform monolayers with a low D-band intensity. The electron mobility of graphene films extracted from field-effect transistor measurements was found to be higher than 4000 $cm^2\ V^{-1}\ s^{-1}$ at room temperature.

Graphene growth by chemical vapor deposition (CVD) has been receiving significant attention recently because of the ease with which large-area films can be grown, but the growth of large-domain or large-grain-size single crystals has not been reported to date.[1] In our earlier work, we found that growth of graphene on Cu by CVD occurs predominantly by surface nucleation followed by a two-dimensional growth process, but the domain size was limited to a few tens of micrometers.[2,3] The presence of domain boundaries has been found to be detrimental to the transport properties; the precise mechanism of the degradation still remains elusive, but what is known is that structural defects promote surface reactions with adsorbates from the ambient or with deposited dielectrics.[3] The presence of heptagons and pentagons in the network of hexagons has been observed experimentally, and first-principles quantum-transport calculations have predicted that the periodicity-breaking disorder can adversely affect transport properties.[4,5] Any of these defects can give rise to higher surface chemical activity that would further disrupt the sp^2-bonding nature of graphene and thus impact graphene's fundamental properties. Therefore, it is imperative that large single crystals of graphene be grown to minimize the presence of defects arising from boundaries between misoriented domains. In this communication, we report a very low pressure CVD process that yields graphene with domains of up to 0.5 mm in size, which is a factor of ~30 times larger than previously reported.[3]

The large-domain graphene growth was observed on the inside of a copper-foil enclosure at high temperature (~1035 °C). The copper-foil enclosure (Figure 1a) was formed by bending a 25 μm thick copper foil and then crimping the three remaining sides. The basic growth conditions were similar to those previously reported[2,3] but employed slightly lower methane flow rates and partial pressures (less than 1 sccm and 50 mTorr, respectively). Graphene grew on both the inside and outside of the Cu enclosure. The graphene growth on the outside showed behavior similar to the graphene growth reported by Li et al.,[3] but there was one difference: at the lower partial pressure and flow rate and at much longer growth times, a higher density of bilayers and trilayers was observed. This will be reported in future work. In contrast, the growth on the inside showed a much lower density of nuclei followed by very large domain growth after extended periods of time (>1 h) and a much lower density of adlayers. At this time, the precise growth conditions inside the enclosure are not well understood. However, we believe that the low density of nuclei is due to the much lower partial pressure of methane and an "improved" environment during growth; that is, the Cu vapor is in static equilibrium, and there is potentially a much lower pressure of unwanted species in our non-ultrahigh vacuum system. Figure 2 shows the average domain branch length (about half the domain size from the center of the domain) as a function of growth time for two methane flow rates, 0.5 and 1.3 sccm, which correspond to methane partial pressure of 8 and 21 mTorr, respectively. During the growth process, the hydrogen flow rate was kept constant at 2 sccm with a partial pressure of 27 mTorr, and the chamber background pressure was 17 mTorr. The graphene domains were very large, as shown by scanning electron microscope (SEM) images (Figure 3a). The domains also tended to have high "edge roughness". The shape of the graphene nuclei in the initial stages of growth showed a hexagonal symmetry (Figure 3b). At first, the graphene domains grew as six-sided polygons, and these eventually grew into very large graphene domains with growing edges resembling dendrites (Figure 3c).

We also employed the carbon isotope-labeling technique to delineate the graphene growth front in order to establish the boundaries between the growing "lobes", the time dependence, and the spatial dependence.[2] In these experiments, the graphene films were grown by alternating the flow of $^{12}CH_4$ and $^{13}CH_4$ every 10 min for a total of 90 min at a flow rate of 0.5 sccm and a corresponding partial pressure of 8 mTorr at 1035 °C. An

Received: November 1, 2010

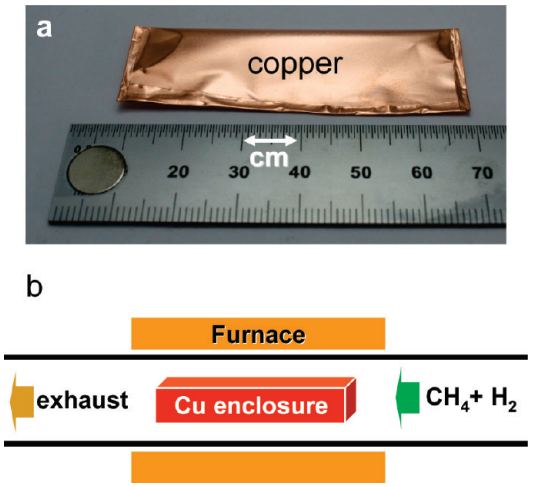

Figure 1. (a) Copper foil enclosure prior to insertion in the furnace. (b) Schematic of the CVD system for graphene on copper.

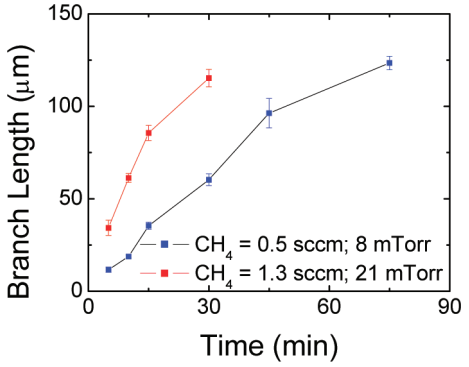

Figure 2. Graphene growth inside the enclosure as a function of time for two methane flow rates and partial pressures at 1035 °C.

analysis of the images in Figure 4 shows that the graphene growth rate was higher at the tips of the lobes (~1.2 μm/min; region 3b) and lower between the lobes and near the end of the growth process (0.1 μm/min; region 7b), as also seen by the spatial coverage variation of graphene. Furthermore, graphene covered the copper surface and closed onto itself as the growth front advanced. The growth rate at points where the graphene joined was lower than at the tip of the growing front. Figure 4 also shows the shape of the growth front at different times during growth, as delineated by the boundaries between the domains of ^{12}C- and ^{13}C-based graphene. The structure of the domains, their distribution, and the graphene growth-front structure provide further indications that the growth was surface-mediated, as previously reported.[2] These data also show that the growth was a result of surface growth on the inside of the enclosure rather than diffusion through the Cu from outside the enclosure followed by precipitation upon cooling.

In order to probe the domain size of the graphene, we made spatially resolved electron diffraction measurements using low-energy electron microscopy (LEEM).[6] Using photoelectron emission microscopy (PEEM), we located the edge of a graphene domain (Figure 5a). We then recorded the diffraction pattern from 2 μm areas of the surface. Diffraction from the substrate revealed a highly faceted, rough Cu(100) surface with sharp diffraction spots, while diffraction from the graphene was diffuse (Figure 5b−e). The diffuse pattern was similar to that for

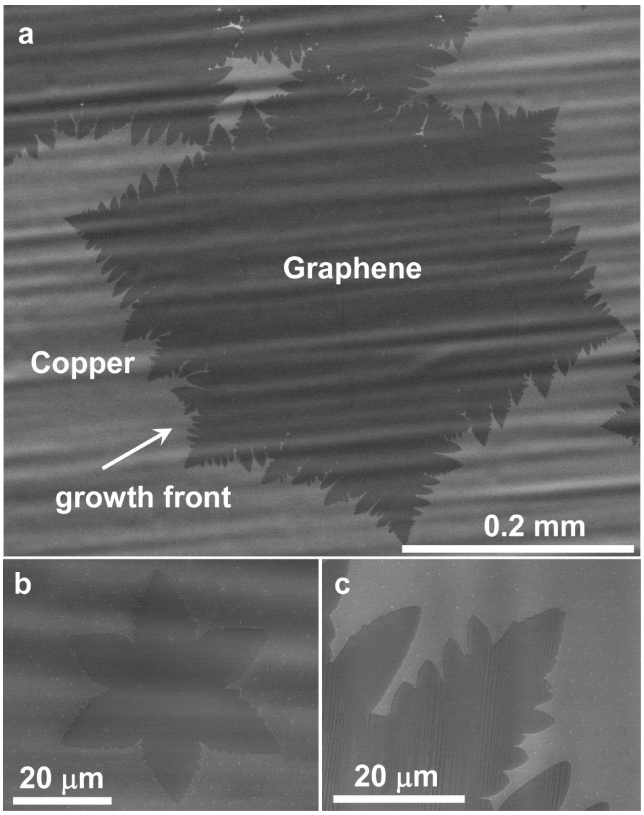

Figure 3. SEM images of graphene on copper grown by CVD. (a) Graphene domain grown at 1035 °C on Cu at an average growth rate of ~6 μm/min. (b) Graphene nuclei formed during the initial stage of growth. (c) High-surface-energy graphene growth front shown by the arrow in (a).

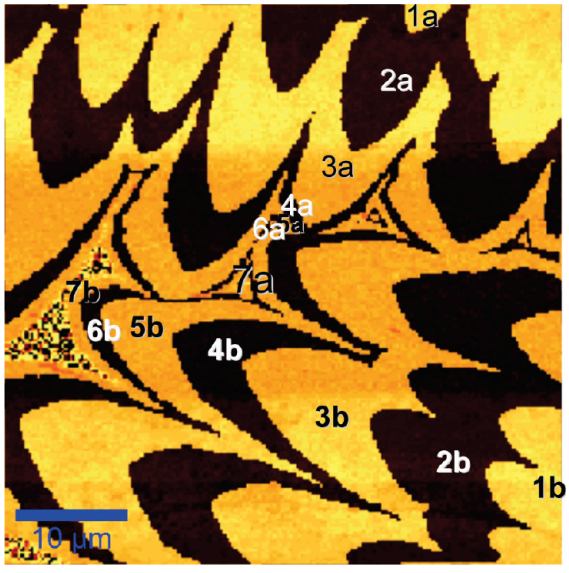

Figure 4. Raman map of the G bands corresponding to ^{12}C (yellow) and ^{13}C (black). The numbers in the figure correspond to the relative methane cycle numbers.

diffraction from free-standing graphene,[7] perhaps indicating a weak coupling to the rough substrate. To estimate the domain size, we recorded the diffraction pattern as the sample was

dx.doi.org/10.1021/ja109793s |J. Am. Chem. Soc. XXXX, XXX, 000–000

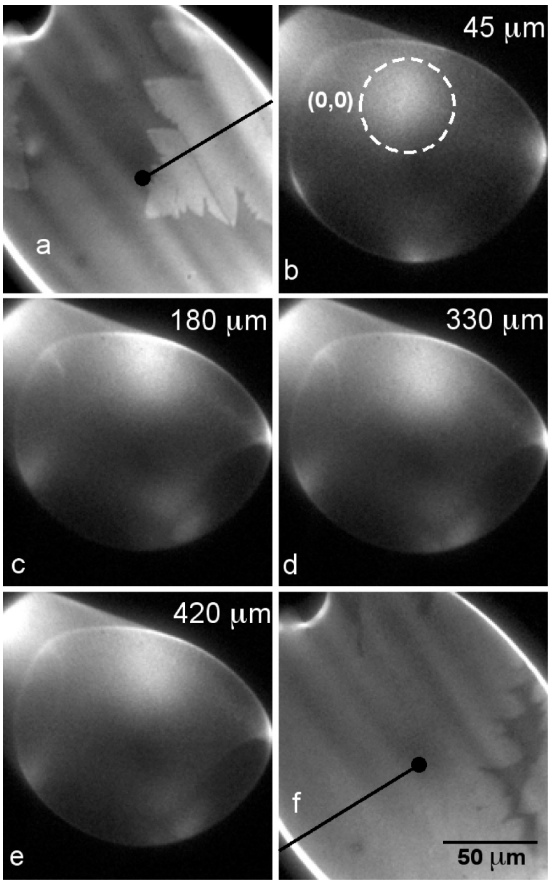

Figure 5. (a) PEEM image recorded near a graphene domain. The black line indicates the path from which selected-area diffraction patterns were recorded. The graphene is bright, and the surrounding Cu foil is dark. (b−e) Electron diffraction patterns (33 eV) recorded from 2 μm areas of the graphene. Each pattern is labeled by the position along the black line in (a) at which the pattern was recorded. The diffraction spots are indicated in (b). (f) PEEM image recorded at the end of the scan.

scanned under the beam along a line at a constant speed of 15 μm/s, and Figure 5 shows the PEEM images and diffraction patterns from selected points along the line scan. Each pattern is labeled by the position from which it was recorded.

While there were slight continuous rotations of the pattern due to waviness in the foil, there were no discontinuous changes in the orientation of the diffraction spots, suggesting that along this scan of over 400 μm, there were no rotational domain boundaries. We performed similar measurements on a number of domains. On occasion, we observed large (>50 μm) domains with a 30 degree relative rotation of the graphene lattice, but in most of the scans, no rotational domain boundaries were observed.

After growth, the graphene films were transferred to SiO_2/Si substrates as described by Li et al.[8] in order to analyze the films by Raman spectroscopy and perform electrical measurements. Figure 6 shows Raman maps of the D band (Figure 6a) and G band (Figure 6b) and Raman spectra recorded at two different regions of the domain (Figure 6c), one within the film and the other close to the dendrite edge. The spectra show that the growing material was indeed graphene, with a low D band intensity across the domain and the presence of graphene only. The full width at half-maximum (FWHM) of the G band was about the same for the two regions (23 cm^{-1}), and the intensity ratio of

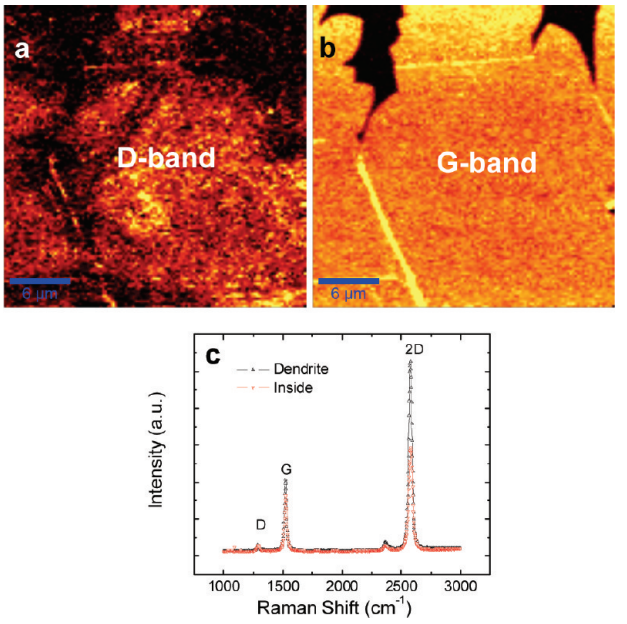

Figure 6. (a) D-band and (b) G-band Raman maps of graphene within the domain and at the edges of the growing domain and (c) Raman spectra of large-domain graphene within the bulk of the film and along the dendrite. The FWHM of the 2D band of the dendrite was slightly smaller than that of the bulk, and the ratio of the intensities of the 2D and G bands was larger for the dendritic region than the bulk, suggesting a lower carrier concentration for the dendritic region within the "bulk" of the domain and the tip of the dendrite. The 2D peak FWHM was 38 cm^{-1} for the bulk and 32 cm^{-1} for the dendrite, whereas the G-band FWHM was ~23 cm^{-1} for both regions.

the 2D band to the G band suggests that the carrier concentration was different for the two regions.[9] This variation will have to be investigated further.

The quality of the large-area-domain films was also evaluated by measuring the transport properties of the graphene films transferred onto silicon dioxide grown on Si wafers. Field-effect transistors were fabricated using nickel for the source and drain contacts and the highly doped Si substrate as the back-gate contact. The resistance was measured at room temperature as a function of back-gate voltage, and the mobility was extracted using the methodology introduced by Kim et al.[10] The mobility for these large-domain films was found to be greater than 4000 $cm^2\ V^{-1}\ s^{-1}$, which is reasonably high but not as high as the highest value for exfoliated films, thus suggesting that the films still need improvement.

AUTHOR INFORMATION

Corresponding Author
colombo@ti.com; r.ruoff@mail.utexas.edu

ACKNOWLEDGMENT

The authors appreciate the support from the Nanoelectronic Research Initiative—SouthWest Academy of Nanoelectronics (NRI-SWAN), NSF Grant 1006350, and the Office of Naval Research.

REFERENCES

(1) Li, X.; Cai, W.; An, J. H.; Kim, S.; Nah, J.; Yang, D.; Piner, R.; Velamakanni, A.; Jung, I.; Tutuc, E.; Banerjee, S. K.; Colombo, L.; Ruoff, R. S. *Science* **2009**, *324*, 1312–1314.

dx.doi.org/10.1021/ja109793s |*J. Am. Chem. Soc.* XXXX, XXX, 000–000

(2) Li, X.; Cai, W.; Colombo, L.; Ruoff, R. S. *Nano Lett.* **2009**, *9*, 4268–4272.
(3) Li, X.; Magnuson, C. W.; Venugopal, A.; An, J.; Suk, J. W.; Han, B.; Borysiak, M.; Cai, W.; Velamakanni, A.; Zhu, Y.; Fu, L.; Vogel, E. M.; Voelkl, E.; Colombo, L.; Ruoff, R. S. *Nano Lett.* **2010**, *10*, 4328–34.
(4) Huang, P. Y.; Ruiz-Vargas, C. S.; Zande, A. M.; Whitney, W. S.; Garg, S.; Alden, J. S.; Hustedt, C. J.; Zhu, Y.; Park, J.; McEuen, P. L.; Muller, D. A. *Nature* **2011**, *469*, 389–392.
(5) Yazyev, O. V.; Louie, S. G. *Nat. Mater.* **2010**, *9*, 806–809.
(6) Bauer, E. *Rep. Prog. Phys.* **1994**, *57*, 895–938.
(7) Knox, K. R.; Wang, S.; Morgante, A.; Cvetko, D.; Locatelli, A.; Mentes, T. O.; Nino, M. A.; Kim, P.; Osgood, R. M. *Phys. Rev. B* **2008**, *78*, No. 201408.
(8) Li, X.; Zhu, Y.; Cai, W.; Borysiak, M.; Han, B.; Chen, D.; Piner, R. D.; Colombo, L.; Ruoff, R. S. *Nano Lett.* **2009**, *9*, 4359–4363.
(9) Casiraghi, C.; Pisana, S.; Novoselov, K. S.; Geim, A. K.; Ferrari, A. C. *Appl. Phys. Lett.* **2007**, *91*, No. 233108.
(10) Kim, S.; Nah, J.; Jo, I.; Shahrjerdi, D.; Colombo, L.; Yao, Z.; Tutuc, E.; Banerjee, S. K. *Appl. Phys. Lett.* **2009**, *94*, No. 062107.